

ISSN 1726-5479

SENSORS & TRANSDUCERS

3 vol. 14-1
Special
/12



Physical and Chemical Sensors & Wireless Sensor Networks

International Frequency Sensor Association Publishing



Editors-in-Chief: Sergey Y. Yurish, tel.: +34 93 413 7941, e-mail: editor@sensorsportal.com

Editors for Western Europe

Meijer, Gerard C.M., Delft University of Technology, The Netherlands
Ferrari, Vittorio, Università di Brescia, Italy

Editor for Eastern Europe

Sachenko, Anatoly, Ternopil State Economic University, Ukraine

Editors for North America

Datskos, Panos G., Oak Ridge National Laboratory, USA
Fabien, J. Josse, Marquette University, USA
Katz, Evgeny, Clarkson University, USA

Editor South America

Costa-Felix, Rodrigo, Inmetro, Brazil

Editor for Africa

Maki K.Habib, American University in Cairo, Egypt

Editor for Asia

Ohyama, Shinji, Tokyo Institute of Technology, Japan

Editor for Asia-Pacific

Mukhopadhyay, Subhas, Massey University, New Zealand

Editorial Advisory Board

- Abdul Rahim, Ruzairi, Universiti Teknologi, Malaysia
Ahmad, Mohd Noor, Nothern University of Engineering, Malaysia
Annamalai, Karthigeyan, National Institute of Advanced Industrial Science and Technology, Japan
Arcega, Francisco, University of Zaragoza, Spain
Arguel, Philippe, CNRS, France
Ahn, Jae-Pyoung, Korea Institute of Science and Technology, Korea
Arndt, Michael, Robert Bosch GmbH, Germany
Ascoli, Giorgio, George Mason University, USA
Atalay, Selcuk, Inonu University, Turkey
Atghiaee, Ahmad, University of Tehran, Iran
Augutis, Vyantas, Kaunas University of Technology, Lithuania
Avachit, Patil Lalchand, North Maharashtra University, India
Ayesh, Aladdin, De Montfort University, UK
Azamimi, Azian binti Abdullah, Universiti Malaysia Perlis, Malaysia
Bahreyni, Behraad, University of Manitoba, Canada
Baliga, Shankar, B., General Monitors Transnational, USA
Baoxian, Ye, Zhengzhou University, China
Barford, Lee, Agilent Laboratories, USA
Barlingay, Ravindra, RF Arrays Systems, India
Basu, Sukumar, Jadavpur University, India
Beck, Stephen, University of Sheffield, UK
Ben Bouzid, Sihem, Institut National de Recherche Scientifique, Tunisia
Benachaiba, Chellali, Universitaire de Bechar, Algeria
Binnie, T. David, Napier University, UK
Bischoff, Gerlinde, Inst. Analytical Chemistry, Germany
Bodas, Dhananjay, IMTEK, Germany
Borges Carval, Nuno, Universidade de Aveiro, Portugal
Bouchikhi, Benachir, University Moulay Ismail, Morocco
Bousbia-Salah, Mounir, University of Annaba, Algeria
Bouvet, Marcel, CNRS – UPMC, France
Brudzewski, Kazimierz, Warsaw University of Technology, Poland
Cai, Chenxin, Nanjing Normal University, China
Cai, Qingyun, Hunan University, China
Calvo-Gallego, Jaime, Universidad de Salamanca, Spain
Campanella, Luigi, University La Sapienza, Italy
Carvalho, Vitor, Minho University, Portugal
Cecelja, Franjo, Brunel University, London, UK
Cerde Belmonte, Judith, Imperial College London, UK
Chakrabarty, Chandan Kumar, Universiti Tenaga Nasional, Malaysia
Chakravorty, Dipankar, Association for the Cultivation of Science, India
Changhai, Ru, Harbin Engineering University, China
Chaudhari, Gajanan, Shri Shivaji Science College, India
Chavali, Murthy, N.I. Center for Higher Education, (N.I. University), India
Chen, Jiming, Zhejiang University, China
Chen, Rongshun, National Tsing Hua University, Taiwan
Cheng, Kuo-Sheng, National Cheng Kung University, Taiwan
Chiang, Jeffrey (Cheng-Ta), Industrial Technol. Research Institute, Taiwan
Chiriac, Horia, National Institute of Research and Development, Romania
Chowdhuri, Arijit, University of Delhi, India
Chung, Wen-Yaw, Chung Yuan Christian University, Taiwan
Corres, Jesus, Universidad Publica de Navarra, Spain
Cortes, Camilo A., Universidad Nacional de Colombia, Colombia
Courtois, Christian, Université de Valenciennes, France
Cusano, Andrea, University of Sannio, Italy
D'Amico, Arnaldo, Università di Tor Vergata, Italy
De Stefano, Luca, Institute for Microelectronics and Microsystem, Italy
Deshmukh, Kiran, Shri Shivaji Mahavidyalaya, Barshi, India
Dickert, Franz L., Vienna University, Austria
Dieguez, Angel, University of Barcelona, Spain
Dighavkar, C. G., M.G. Vidyamandir's L. V.H. College, India
Dimitropoulos, Panos, University of Thessaly, Greece
Ding, Jianning, Jiangsu Polytechnic University, China
Djordjevic, Alexandar, City University of Hong Kong, Hong Kong
Donato, Nicola, University of Messina, Italy
Donato, Patricio, Universidad de Mar del Plata, Argentina
Dong, Feng, Tianjin University, China
Drljaca, Predrag, Intersema Sensoric SA, Switzerland
Dubey, Venketesh, Bournemouth University, UK
Enderle, Stefan, Univ. of Ulm and KTB Mechatronics GmbH, Germany
Erdem, Gursan K. Arzum, Ege University, Turkey
Erkmen, Aydan M., Middle East Technical University, Turkey
Estelle, Patrice, Insa Rennes, France
Estrada, Horacio, University of North Carolina, USA
Faiz, Adil, INSA Lyon, France
Fericean, Sorin, Balluff GmbH, Germany
Fernandes, Joana M., University of Porto, Portugal
Francioso, Luca, CNR-IMM Institute for Microelectronics and Microsystems, Italy
Francis, Laurent, University Catholique de Louvain, Belgium
Fu, Weiling, South-Western Hospital, Chongqing, China
Gaura, Elena, Coventry University, UK
Geng, Yanfeng, China University of Petroleum, China
Gole, James, Georgia Institute of Technology, USA
Gong, Hao, National University of Singapore, Singapore
Gonzalez de la Rosa, Juan Jose, University of Cadiz, Spain
Granel, Annette, Goteborg University, Sweden
Graff, Mason, The University of Texas at Arlington, USA
Guan, Shan, Eastman Kodak, USA
Guillet, Bruno, University of Caen, France
Guo, Zhen, New Jersey Institute of Technology, USA
Gupta, Narendra Kumar, Napier University, UK
Hadjiloucas, Sillas, The University of Reading, UK
Haider, Mohammad R., Sonoma State University, USA
Hashsham, Syed, Michigan State University, USA
Hasni, Abdelhafid, Bechar University, Algeria
Hernandez, Alvaro, University of Alcala, Spain
Hernandez, Wilmar, Universidad Politecnica de Madrid, Spain
Homontcovschi, Dorel, SUNY Binghamton, USA
Horstman, Tom, U.S. Automation Group, LLC, USA
Hsiai, Tzung (John), University of Southern California, USA
Huang, Jeng-Sheng, Chung Yuan Christian University, Taiwan
Huang, Star, National Tsing Hua University, Taiwan
Huang, Wei, PSG Design Center, USA
Hui, David, University of New Orleans, USA
Jaffrezic-Renault, Nicole, Ecole Centrale de Lyon, France
James, Daniel, Griffith University, Australia
Janting, Jakob, DELTA Danish Electronics, Denmark
Jiang, Liudi, University of Southampton, UK
Jiang, Wei, University of Virginia, USA
Jiao, Zheng, Shanghai University, China
John, Joachim, IMEC, Belgium
Kalach, Andrew, Voronezh Institute of Ministry of Interior, Russia
Kang, Moonho, Sunmoon University, Korea South
Kaniusas, Eugenijus, Vienna University of Technology, Austria
Katake, Anup, Texas A&M University, USA
Kausel, Wilfried, University of Music, Vienna, Austria
Kavasoglu, Nese, Mugla University, Turkey
Ke, Cathy, Tyndall National Institute, Ireland
Khelfaoui, Rachid, Université de Bechar, Algeria
Khan, Asif, Aligarh Muslim University, Aligarh, India
Kim, Min Young, Kyungpook National University, Korea South
Ko, Sang Choon, Electronics. and Telecom. Research Inst., Korea South
Kotulska, Malgorzata, Wroclaw University of Technology, Poland
Kockar, Hakan, Balikesir University, Turkey

Kong, Ing, RMIT University, Australia
Kratz, Henrik, Uppsala University, Sweden
Krishnamoorthy, Ganesh, University of Texas at Austin, USA
Kumar, Arun, University of Delaware, Newark, USA
Kumar, Subodh, National Physical Laboratory, India
Kung, Chih-Hsien, Chang-Jung Christian University, Taiwan
Lacnjevac, Caslav, University of Belgrade, Serbia
Lay-Ekuakille, Aime, University of Lecce, Italy
Lee, Jang Myung, Pusan National University, Korea South
Lee, Jun Su, Amkor Technology, Inc. South Korea
Lei, Hua, National Starch and Chemical Company, USA
Li, Fengyuan (Thomas), Purdue University, USA
Li, Genxi, Nanjing University, China
Li, Hui, Shanghai Jiaotong University, China
Li, Xian-Fang, Central South University, China
Li, Yuefa, Wayne State University, USA
Liang, Yuanchang, University of Washington, USA
Liawruangrath, Saisunee, Chiang Mai University, Thailand
Liew, Kim Meow, City University of Hong Kong, Hong Kong
Lin, Hermann, National Kaohsiung University, Taiwan
Lin, Paul, Cleveland State University, USA
Linderholm, Pontus, EPFL - Microsystems Laboratory, Switzerland
Liu, Aihua, University of Oklahoma, USA
Liu Changgeng, Louisiana State University, USA
Liu, Cheng-Hsien, National Tsing Hua University, Taiwan
Liu, Songqin, Southeast University, China
Lodeiro, Carlos, University of Vigo, Spain
Lorenzo, Maria Encarnacio, Universidad Autonoma de Madrid, Spain
Lukaszewicz, Jerzy Pawel, Nicholas Copernicus University, Poland
Ma, Zhanfang, Northeast Normal University, China
Majstorovic, Vidosav, University of Belgrade, Serbia
Malyshev, V.V., National Research Centre 'Kurchatov Institute', Russia
Marquez, Alfredo, Centro de Investigacion en Materiales Avanzados, Mexico
Matay, Ladislav, Slovak Academy of Sciences, Slovakia
Mathur, Prafull, National Physical Laboratory, India
Maurya, D.K., Institute of Materials Research and Engineering, Singapore
Mekid, Samir, University of Manchester, UK
Melnyk, Ivan, Photon Control Inc., Canada
Mendes, Paulo, University of Minho, Portugal
Mennell, Julie, Northumbria University, UK
Mi, Bin, Boston Scientific Corporation, USA
Minas, Graca, University of Minho, Portugal
Moghavvemi, Mahmoud, University of Malaya, Malaysia
Mohammadi, Mohammad-Reza, University of Cambridge, UK
Molina Flores, Esteban, Benemérita Universidad Autónoma de Puebla, Mexico
Moradi, Majid, University of Kerman, Iran
Morello, Rosario, University "Mediterranea" of Reggio Calabria, Italy
Mounir, Ben Ali, University of Sousse, Tunisia
Mrad, Nezih, Defence R&D, Canada
Mulla, Imtiaz Sirajuddin, National Chemical Laboratory, Pune, India
Nabok, Aleksey, Sheffield Hallam University, UK
Neelamegam, Periasamy, Sastra Deemed University, India
Neshkova, Milka, Bulgarian Academy of Sciences, Bulgaria
Oberhammer, Joachim, Royal Institute of Technology, Sweden
Ould Lahoucine, Cherif, University of Guelma, Algeria
Pamidighanta, Sayanu, Bharat Electronics Limited (BEL), India
Pan, Jisheng, Institute of Materials Research & Engineering, Singapore
Park, Joon-Shik, Korea Electronics Technology Institute, Korea South
Penza, Michele, ENEA C.R., Italy
Pereira, Jose Miguel, Instituto Politecnico de Seteбал, Portugal
Petsev, Dimitar, University of New Mexico, USA
Pogacnik, Lea, University of Ljubljana, Slovenia
Post, Michael, National Research Council, Canada
Prance, Robert, University of Sussex, UK
Prasad, Ambika, Gulbarga University, India
Prateepasen, Asa, Kingmoungut's University of Technology, Thailand
Pugno, Nicola M., Politecnico di Torino, Italy
Pullini, Daniele, Centro Ricerche FIAT, Italy
Pumera, Martin, National Institute for Materials Science, Japan
Radhakrishnan, S., National Chemical Laboratory, Pune, India
Rajanna, K., Indian Institute of Science, India
Ramadan, Qasem, Institute of Microelectronics, Singapore
Rao, Basuthkar, Tata Inst. of Fundamental Research, India
Raouf, Kosai, Joseph Fourier University of Grenoble, France
Rastogi Shiva, K., University of Idaho, USA
Reig, Candid, University of Valencia, Spain
Restivo, Maria Teresa, University of Porto, Portugal
Robert, Michel, University Henri Poincare, France
Rezazadeh, Ghader, Urmia University, Iran
Royo, Santiago, Universitat Politècnica de Catalunya, Spain
Rodriguez, Angel, Universidad Politécnica de Cataluña, Spain
Rothberg, Steve, Loughborough University, UK
Sadana, Ajit, University of Mississippi, USA
Sadeghian Marnani, Hamed, TU Delft, The Netherlands
Sapozhnikova, Ksenia, D.I.Mendeleyev Institute for Metrology, Russia
Sandacci, Serghei, Sensor Technology Ltd., UK
Saxena, Vibha, Bhabha Atomic Research Centre, Mumbai, India
Schneider, John K., Ultra-Scan Corporation, USA
Sengupta, Deepak, Advance Bio-Photonics, India
Seif, Selemeni, Alabama A & M University, USA
Seifter, Achim, Los Alamos National Laboratory, USA
Shah, Kriyang, La Trobe University, Australia
Sankarraj, Anand, Detector Electronics Corp., USA
Silva Girao, Pedro, Technical University of Lisbon, Portugal
Singh, V. R., National Physical Laboratory, India
Slomovitz, Daniel, UTE, Uruguay
Smith, Martin, Open University, UK
Soleymanpour, Ahmad, Damghan Basic Science University, Iran
Somani, Prakash R., Centre for Materials for Electronics Technol., India
Sridharan, M., Sastra University, India
Srinivas, Talabattula, Indian Institute of Science, Bangalore, India
Srivastava, Arvind K., NanoSonix Inc., USA
Stefan-van Staden, Raluca-Ioana, University of Pretoria, South Africa
Stefanescu, Dan Mihai, Romanian Measurement Society, Romania
Sumriddetchka, Sarun, National Electronics and Computer Technology Center, Thailand
Sun, Chengliang, Polytechnic University, Hong-Kong
Sun, Dongming, Jilin University, China
Sun, Junhua, Beijing University of Aeronautics and Astronautics, China
Sun, Zhiqiang, Central South University, China
Suri, C. Raman, Institute of Microbial Technology, India
Sysoev, Victor, Saratov State Technical University, Russia
Szewczyk, Roman, Industrial Research Inst. for Automation and Measurement, Poland
Tan, Ooi Kiang, Nanyang Technological University, Singapore
Tang, Dianping, Southwest University, China
Tang, Jaw-Luen, National Chung Cheng University, Taiwan
Teker, Kasif, Frostburg State University, USA
Thirunavukkarasu, I., Manipal University Karnataka, India
Thumbavanam Pad, Kartik, Carnegie Mellon University, USA
Tian, Gui Yun, University of Newcastle, UK
Tsiantos, Vassilios, Technological Educational Institute of Kaval, Greece
Tsigara, Anna, National Hellenic Research Foundation, Greece
Twomey, Karen, University College Cork, Ireland
Valente, Antonio, University, Vila Real, - U.T.A.D., Portugal
Vanga, Raghav Rao, Summit Technology Services, Inc., USA
Vaseashta, Ashok, Marshall University, USA
Vazquez, Carmen, Carlos III University in Madrid, Spain
Vieira, Manuela, Instituto Superior de Engenharia de Lisboa, Portugal
Vigna, Benedetto, STMicroelectronics, Italy
Vrba, Radimir, Brno University of Technology, Czech Republic
Wandelt, Barbara, Technical University of Lodz, Poland
Wang, Jiangping, Xi'an Shiyou University, China
Wang, Kedong, Beihang University, China
Wang, Liang, Pacific Northwest National Laboratory, USA
Wang, Mi, University of Leeds, UK
Wang, Shinn-Fwu, Ching Yun University, Taiwan
Wang, Wei-Chih, University of Washington, USA
Wang, Wensheng, University of Pennsylvania, USA
Watson, Steven, Center for NanoSpace Technologies Inc., USA
Weiping, Yan, Dalian University of Technology, China
Wells, Stephen, Southern Company Services, USA
Wolkenberg, Andrzej, Institute of Electron Technology, Poland
Woods, R. Clive, Louisiana State University, USA
Wu, DerHo, National Pingtung Univ. of Science and Technology, Taiwan
Wu, Zhaoyang, Hunan University, China
Xiu Tao, Ge, Chuzhou University, China
Xu, Lisheng, The Chinese University of Hong Kong, Hong Kong
Xu, Sen, Drexel University, USA
Xu, Tao, University of California, Irvine, USA
Yang, Dongfang, National Research Council, Canada
Yang, Shuang-Hua, Loughborough University, UK
Yang, Wuqiang, The University of Manchester, UK
Yang, Xiaoling, University of Georgia, Athens, GA, USA
Yaping Dan, Harvard University, USA
Ymeti, Aurel, University of Twente, Netherlands
Yong Zhao, Northeastern University, China
Yu, Haihu, Wuhan University of Technology, China
Yuan, Yong, Massey University, New Zealand
Yufra Garcia, Alberto, Seville University, Spain
Zakaria, Zulkarnay, University Malaysia Perlis, Malaysia
Zagnoni, Michele, University of Southampton, UK
Zamani, Cyrus, Universitat de Barcelona, Spain
Zeni, Luigi, Second University of Naples, Italy
Zhang, Minglong, Shanghai University, China
Zhang, Quintao, University of California at Berkeley, USA
Zhang, Weiping, Shanghai Jiao Tong University, China
Zhang, Wenming, Shanghai Jiao Tong University, China
Zhang, Xueji, World Precision Instruments, Inc., USA
Zhong, Haoxiang, Henan Normal University, China
Zhu, Qing, Fujifilm Dimatix, Inc., USA
Zorzano, Luis, Universidad de La Rioja, Spain
Zourob, Mohammed, University of Cambridge, UK

Contents

Volume 14-1
Special Issue
March 2012

www.sensorsportal.com

ISSN 1726-5479

Research Articles

Physical and Chemical Sensors & Wireless Sensor Networks (Foreword) <i>Sergey Y. Yurish, Petre Dini</i>	I
From Smart to Intelligent Sensors: A Case Study <i>Vincenzo Di Lecce, Marco Calabrese</i>	1
Smart Optoelectronic Sensors and Intelligent Sensor Systems <i>Sergey Y. Yurish</i>	18
Accelerometer and Magnetometer Based Gyroscope Emulation on Smart Sensor for a Virtual Reality Application <i>Baptiste Delporte, Laurent Perroton, Thierry Grandpierre and Jacques Trichet</i>	32
Top-Level Simulation of a Smart-Bolometer Using VHDL Modeling <i>Matthieu Denoual and Patrick Attia</i>	48
A Novel Liquid Level Sensor Design Using Laser Optics Technology <i>Mehmet Emre Erdem and Doğan Güneş</i>	65
Recognition of Simple Gestures Using a PIR Sensor Array <i>Piotr Wojtczuk, Alistair Armitage, T. David Binnie, Tim Chamberlain</i>	83
Sinusoidal Calibration of Force Transducers Using Electrodynamic Shaker Systems <i>Christian Schlegel, Gabriela Kiekenap, Bernd Glöckner, Rolf Kumme</i>	95
Experimental Validation of a Sensor Monitoring Ice Formation over a Road Surface <i>Amedeo Troiano, Eros Pasero, Luca Mesin</i>	112
Acoustic Emission Sensing of Structures under Stretch <i>Irinela Chilibon, Marian Mogildea, George Mogildea</i>	122
Differential Search Coils Based Magnetometers: Conditioning, Magnetic Sensitivity, Spatial Resolution <i>Timofeeva Maria, Allegre Gilles, Robbes Didier, Flament Stéphane</i>	134
Silicon Photomultipliers: Dark Current and its Statistical Spread <i>Roberto Pagano, Sebania Libertino, Giusy Valvo, Alfio Russo, Delfo Nunzio Sanfilippo, Giovanni Condorelli, Clarice Di Martino, Beatrice Carbone, Giorgio Fallica and Salvatore Lombardo</i>	151
An Integrated Multimodal Sensor for the On-site Monitoring of the Water Content and Nutrient Concentration of Soil by Measuring the Phase and Electrical Conductivity <i>Masato Futagawa, Md. Iqramul Hussain, Keita Kamado, Fumihiro Dasai, Makoto Ishida, Kazuaki Sawada</i>	160
Design and Evaluation of Impedance Based Sensors for Micro-condensation Measurement under Field and Climate Chamber Conditions <i>Geert Brokmann, Michael Hintz, Barbara March and Arndt Steinke</i>	174

A Parallel Sensing Technique for Automatic Bilayer Lipid Membrane Arrays Monitoring <i>Michele Rossi, Federico Thei and Marco Tartagni</i>	185
Development of Acoustic Devices Functionalized with Cobalt Corroles or Metalloporphyrines for the Detection of Carbon Monoxide at Low Concentration <i>Meddy Vanotti, Virginie Blondeau-Patissier, David Rabus, Jean-Yves Rauch, Jean-Michel Barbe, Sylvain Ballandras</i>	197
Group IV Materials for High Performance Methane Sensing in Novel Slot Optical Waveguides at 2.883 μm and 3.39 μm <i>Vittorio M. N. Passaro, Benedetto Troia and Francesco De Leonardis</i>	212
The Impact of High Dielectric Permittivity on SOI Double-Gate Mosfet Using Nextnano Simulator <i>Samia Slimani, Bouaza Djellouli</i>	231
A Novel Sensor for VOCs Using Nanostructured ZnO and MEMS Technologies <i>H. J. Pandya, Sudhir Chandra and A. L. Vyas</i>	244
$\text{La}_{0.7}\text{Sr}_{0.3}\text{MnO}_3$ Thin Films for Magnetic and Temperature Sensors at Room Temperature <i>Sheng Wu, Dalal Fadil, Shuang Liu, Ammar Aryan, Benoît Renault, Jean-Marc Routoure, Bruno Guillet, Stéphane Flament, Pierre Langlois and Laurence Méchin</i>	253
Cell-Culture Real Time Monitoring Based on Bio-Impedance Measurements <i>Paula Daza, Daniel Cañete, Alberto Olmo, Juan A. García and Alberto Yúfera</i>	266

Authors are encouraged to submit article in MS Word (doc) and Acrobat (pdf) formats by e-mail: editor@sensorsportal.com
Please visit journal's webpage with preparation instructions: <http://www.sensorsportal.com/HTML/DIGEST/Submission.htm>

International Frequency Sensor Association (IFSA).

BioMEMS 2010

Yole's BioMEMS report 2010-2015

IFSA offers
a SPECIAL PRICE

Microsystems Devices Driving Healthcare Applications

The BioMEMS 2010 report is a robust analysis of the Micro Devices with the most advances to develop solutions for vital bio-medical applications. The devices considered are:

Pressure sensors	Microfluidic chips
Silicon microphones	Microdispensers for drug delivery
Accelerometers	Flow meters
Gyroscopes	Infrared temperature sensors
Optical MeMs and image sensors	Emerging MeMs (rfID, strain sensors, energy harvesting)

Also addressed are the regulation aspects for medical device development.

<http://www.sensorsportal.com/HTML/BioMEMS.htm>



The 3rd International Conference on Sensor Device Technologies and Applications



SENSORDEVICES 2012

19 - 24 August 2012 - Rome, Italy

Deadline for papers: 5 April 2012



Tracks: Sensor devices - Ultrasonic and Piezosensors - Photonics - Infrared - Geosensors - Sensor device technologies - Sensors signal conditioning and interfacing circuits - Medical devices and sensors applications - Sensors domain-oriented devices, technologies, and applications - Sensor-based localization and tracking technologies

<http://www.iaria.org/conferences2012/SENSORDEVICES12.html>

The 6th International Conference on Sensor Technologies and Applications



SENSORCOMM 2012

19 - 24 August 2012 - Rome, Italy

Deadline for papers: 5 April 2012



Tracks: Architectures, protocols and algorithms of sensor networks - Energy, management and control of sensor networks - Resource allocation, services, QoS and fault tolerance in sensor networks - Performance, simulation and modelling of sensor networks - Security and monitoring of sensor networks - Sensor circuits and sensor devices - Radio issues in wireless sensor networks - Software, applications and programming of sensor networks - Data allocation and information in sensor networks - Deployments and implementations of sensor networks - Under water sensors and systems - Energy optimization in wireless sensor networks

<http://www.iaria.org/conferences2012/SENSORCOMM12.html>

The 5th International Conference on Advances in Circuits, Electronics and Micro-electronics



CENICS 2012

19 - 24 August 2012 - Rome, Italy

Deadline for papers: 5 April 2012



Tracks: Semiconductors and applications - Design, models and languages - Signal processing circuits - Arithmetic computational circuits - Microelectronics - Electronics technologies - Special circuits - Consumer electronics - Application-oriented electronics

<http://www.iaria.org/conferences2012/CENICS12.html>

La_{0.7}Sr_{0.3}MnO₃ Thin Films for Magnetic and Temperature Sensors at Room Temperature

Sheng Wu, Dalal Fadil, Shuang Liu, Ammar Aryan, Benoit Renault, Jean-Marc Routoure, Bruno Guillet, Stéphane Flament, Pierre Langlois and Laurence Méchin

Université de Caen Basse-Normandie, UMR 6072 GREYC, F-14032 Caen, France

ENSICAEN, UMR 6072 GREYC, F-14050 Caen, France

CNRS, UMR 6072 GREYC, F-14032 Caen, France

E-mail: laurence.mechin@ensicaen.fr

Received: 16 November 2011 /Accepted: 20 December 2011 /Published: 12 March 2012

Abstract: In this paper, the potentialities of the manganese oxide La_{0.7}Sr_{0.3}MnO₃ (LSMO) for the realization of sensitive room temperature thermometers and magnetic sensors are discussed. LSMO exhibits both a large change of the resistance versus temperature at its metal-to-insulator transition (about 330 K) and low field magnetoresistive effects at room temperature. The sensor performances are described in terms of signal-to-noise ratio in the 1 Hz - 100 kHz frequency range. It is shown that due to the very low 1/f noise level, LSMO based sensors can exhibit competitive performances at room temperature. *Copyright © 2012 IFSA.*

Keywords: Low frequency noise, Magnetoresistance sensors, Thermometers.

1. Introduction

Due to the colossal magnetoresistance effect and the strong spin polarization at the Fermi level, the rare earth manganese oxides may find important applications in magnetoresistive devices such as magnetic random access memories and magnetic sensors [1, 2]. In addition, the large change of their electrical resistance R at the metal-to-insulator transition, which takes place in the 300 - 350 K range makes them potential materials for the fabrication of room temperature thermometers. Ideal materials would indeed present at the desired operating temperature T close to 300 K:

- i) a high temperature coefficient of the resistance (β_T), expressed in K^{-1} and defined as the relative derivative of the resistance versus temperature $\beta_T = (1/R) \times (dR/dT)$, or a high relative change of the resistance with the magnetic field (β_H), expressed in T^{-1} , and defined as $\beta_H = (1/R) \times (dR/d(\mu_0 H))$ (with μ_0 the vacuum permeability), and
- ii) a low noise level.

The limits of the device performances are given by the signal-to-noise ratio.

Temperature coefficient of the resistance values and operating temperatures are important parameters to be considered in the fabrication of high sensitivity room-temperature thermometers or magnetoresistances. However, more attention should be paid to the low-frequency noise level in these materials since it can vary by several orders of magnitude while β_H or β_T values may only vary by a factor less than 10. However noise is more difficult to optimize since its origin is still not well known [3-8]. To reduce noise, high material quality is required and a large number of measurements are needed in order to determine the general trend for the evolution of noise with geometrical parameters such as width, length, and sample thickness.

Even if it does not exhibit the highest β_H or β_T values, $La_{0.7}Sr_{0.3}MnO_3$ (LSMO) has been selected among all the possible manganite compositions because it has shown the lowest reported low-frequency noise level so far [8-10].

In this paper, details about sample preparation are presented in section 2. In section 3, the low frequency noise measurement set-up is presented. A discussion about the sensor performances as a function of the geometry, of the bias condition and of the frequency is given in section 4. The performances of LSMO based thermometers as well as magnetoresistive sensors are finally presented and compared with published values.

2. Sample Preparation

The sensors are patterned in 100 nm thick LSMO thin films deposited by pulsed laser deposition from a stoichiometric target onto $SrTiO_3$ (001) single crystal substrate. The laser radiation energy density, the target-to-substrate distance, the oxygen pressure and the substrate temperature were 220 mJ, 50 mm, 0.35 mTorr and 720 °C, respectively.

The deposition conditions were found optimal for producing single-crystalline films as judged by X-ray diffraction. The X-ray diffraction study indicated a full (001) orientation of the LSMO films as shown by the θ - 2θ scan of Fig. 1. Full Width at Half Maximum measured in a ω -scan configuration around the LSMO 002 peak was 0.2° .

An Atomic Force microscopy (AFM) study was performed in tapping mode. As shown in Fig. 2, we observed very smooth surface (with rms roughness of 0.2 nm) and terraces at the film surface.

Electrical resistivity and saturated magnetization were measured in the unpatterned film. They are reported in Fig. 3. Both resistivity and saturated magnetization values are close to those measured in bulk LSMO, thus confirming the overall good quality of the tested sample.

After LSMO deposition, a 200 nm thick gold layer was sputtered on the films in order to make low resistive connections. The LSMO thin films were patterned by UV photolithography and argon ion etching to form lines. As shown in Fig. 4, the mask enables the study of lines of four different widths $W = 20, 50, 100$ and $150 \mu m$. For each width, five lengths L could be measured depending on the

position of the voltage contacts $L = 50, 100, 150, 200$, and $300 \mu\text{m}$. Tens of samples with different geometries have been investigated. In this paper, we chose to report typical results for $50 \mu\text{m}$ wide $300 \mu\text{m}$ long line patterned in a 100 nm thick LSMO film.

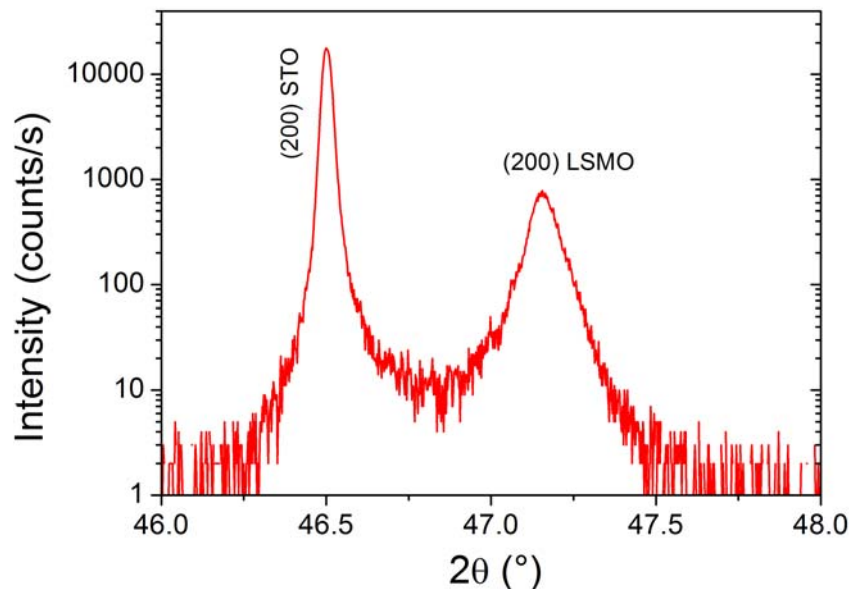


Fig. 1. X-ray diffraction pattern in the θ - 2θ configuration of the 100 nm thick LSMO films on STO(001).

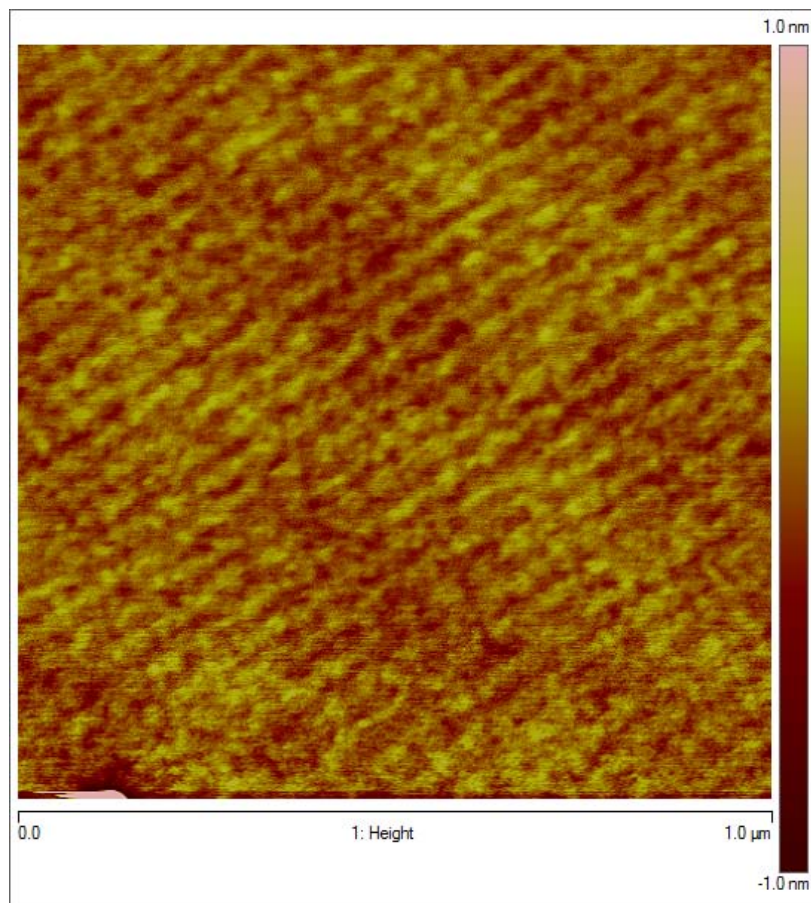


Fig. 2. $1 \mu\text{m} \times 1 \mu\text{m}$ AFM image in tapping mode of the 100 nm thick LSMO film on STO (001).

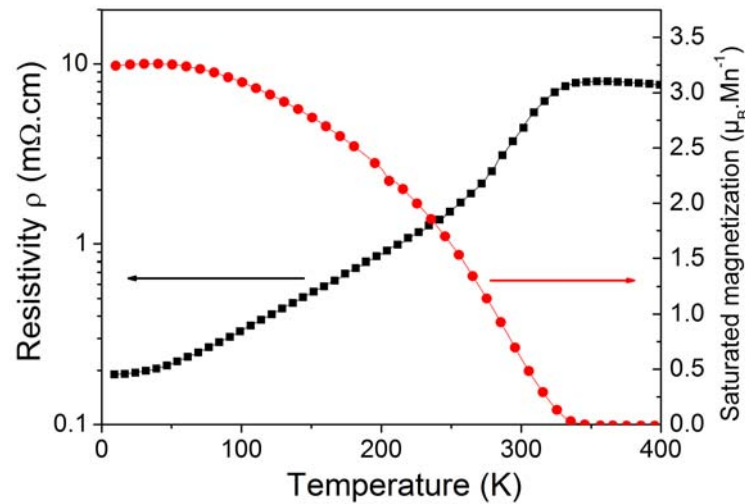


Fig. 3. Electrical resistivity (left axis – black squares) and saturated magnetization in 500 Oe (right axis – red circles) versus temperature of the 100 nm thick LSMO film deposited on STO (001).

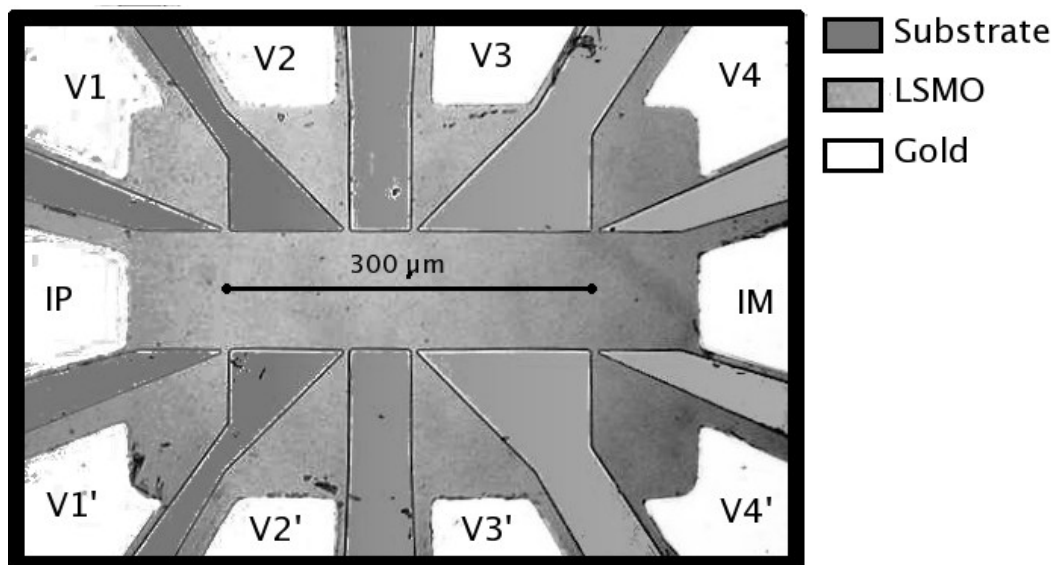


Fig. 4. Optical photography of a 100 μm width line with the two current probes IP and IM and 4 voltage probes (V1...V4, V1'...V4') on each side of the line. The line lengths between V1 - V2, V2 - V3 and V3 - V4 are 100 μm , 50 μm and 150 μm , respectively.

3. Low Frequency Noise Measurements

3.1. Measurement Set-up and Protocol

The experimental set-up mainly consists in one low noise high output impedance DC current source and a dedicated low noise instrumentation amplifier with the following characteristics: a DC output dedicated to resistance measurement with a voltage gain equal to 10 and an AC output dedicated to noise measurements with a voltage gain around one thousand and a 1 Hz - 1 MHz bandwidth [11]. The input voltage white noise is around $20 \times 10^{-18} \text{ V}^2 \cdot \text{Hz}^{-1}$ and its input current noise is negligible. The device is connected at the output of the DC current source using IP and IM pads (defined in Figs. 4 and 5). The DC voltage as well as the voltage noise are measured using the instrumentation amplifier connected either on IP, IM pads for two probe configuration or on V_i, V_j ($i, j=1..4$ with $i \neq j$) for four

probe configuration. A spectrum analyzer Agilent 89410A calculates the noise spectral density for frequencies in the 1 Hz - 1 MHz range.

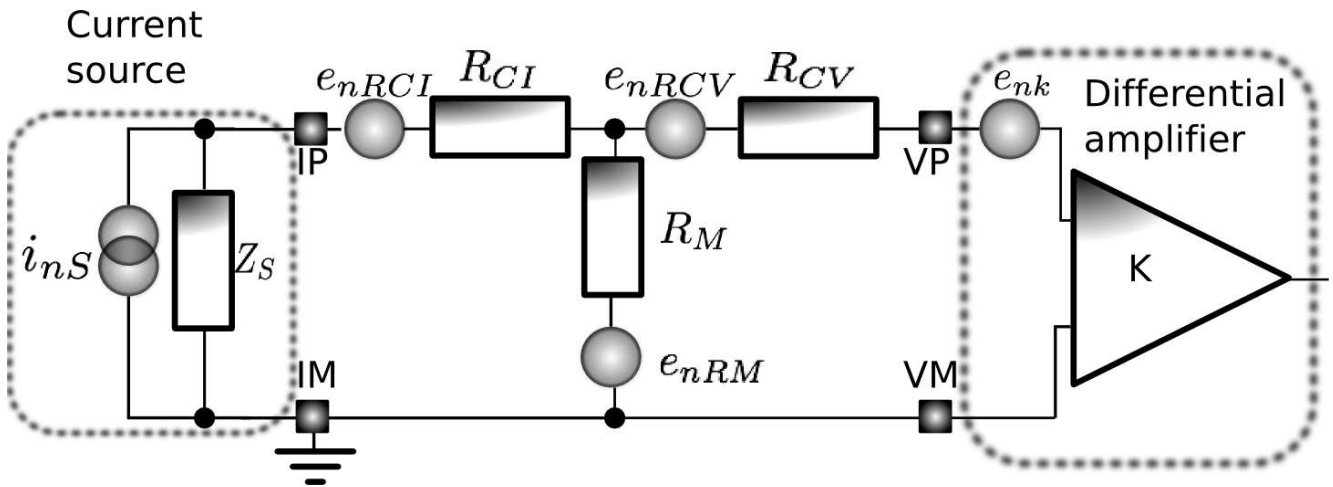


Fig. 5. Schematic representation of the noise measurement set-up showing the four probe technique. The noise sources are located for the current source, the sample and the differential amplifier. Z_S is the output impedance of the current source, R_{CI} is the current contact resistance (for simplicity, R_{CI} is the sum of then current contact resistance of the two probes I_P and I_M), R_M is the film resistance, R_{CV} is the voltage contact resistance (R_{CV} is the sum of the voltage contact resistance of the two probes V_P and V_M), i_{nS} is the current source noise, e_{nRCI} is the current contact resistance noise, e_{nRM} is the film noise, e_{nRCV} is the voltage contact resistance noise and e_{nk} is the differential amplifier noise of spectral density.

According to [11], the DC current source is quasi-ideal, i.e. its output impedance is infinite and its noise contribution is negligible. It is also assumed that the input impedance of the instrumentation amplifier is very high so that no DC current flows in its inputs. It will be also considered that the noise contribution of the amplifier is known and can be subtracted from the measured noise when a device is connected at its input. The noise of the measurement set-up is deduced from the measurement performed at zero bias. This set-up contribution is then removed from all the measured data with applied bias current.

Fig. 6 shows the noise spectral density measured in the two probes (S_{V2p}) and the four probe configurations (S_{V4p}) for the same DC current I . Two noise contributions were found: a white noise one and a $1/f$ noise one. The white noise level is clearly due the thermal noise contribution given by $4k_BTR$ (k_B is the Boltzmann constant equal to $1.38 \times 10^{-23} \text{ J}\cdot\text{K}^{-1}$) and should not depend on the bias current. The white noise level is consistent with the expected value deduced from the DC measurement of the sample resistance thus validating the thermal origin of the white noise. One should notice that thermal noise of the voltage contact should have to be taken into account but for simplicity, this contribution as well as the amplifier noise will be neglected in the following: optimal sensor geometries (especially for the voltage contact) and optimized read-out electronic may easily be used to fulfil this requirement indeed.

Different noise contributions that both generate white noise and $1/f$ noise have to be considered in the sensor: the voltage contact noise, the current contact noise and the film noise (as shown in Fig. 5). Details can be found in [12]. It can be shown that in the two probe configuration, both film and current contact noise contributions are measured. In the four probe configuration, due to the high output impedance of the DC current source, the current contact noise contribution can be completely eliminated. Since no DC current flows into the voltage contact, one would assume that no $1/f$ noise exists for the voltage contact sources. As shown in Fig. 6, in the four probe configuration (i.e. when

the amplifier is connected to the VP, VM pads), the measured spectral density S_{V4p} is the sample noise spectral density without any correction whereas in the two probe configuration (when the amplifier is connected to the IP and IM pads), the measured spectral density S_{V2p} is the sum of the current contact noise and the sample noise spectral densities.

The contact contribution originates from the contact between gold and LSMO and thus presents a great impact for sensor applications. Fig. 6 also shows that for this sample, the current contact contribution is much higher than the film noise. This result has already been reported by other studies [13]. It can lead to an overestimation of the film noise if the current source used for the measurement does not exhibit large output impedance.

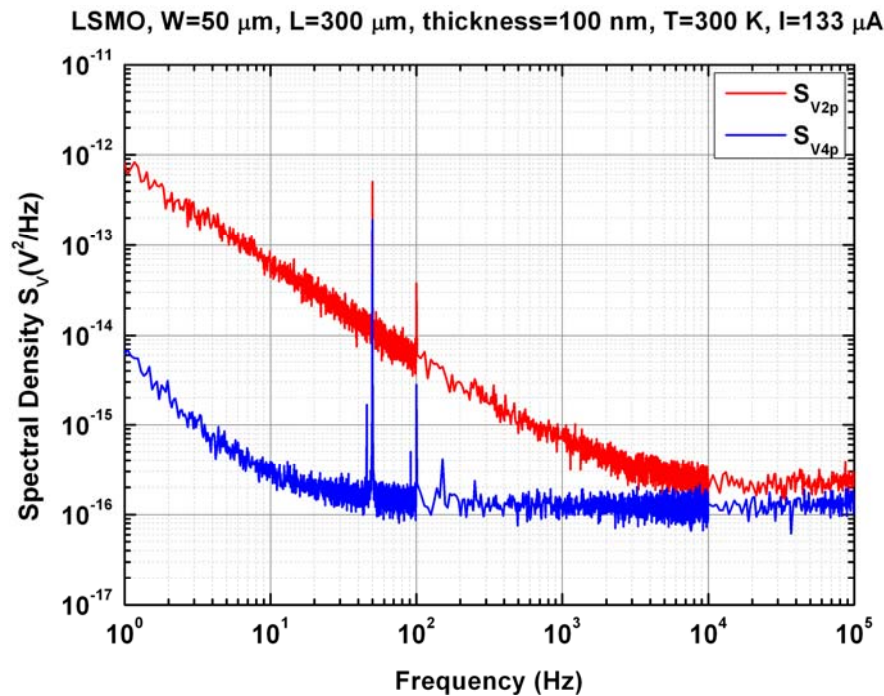


Fig. 6. Noise spectral densities in the two probes (S_{V2p}) and the four probe (S_{V4p}) configurations for the same DC bias current. Using the mask shown in Fig. 4, the current contact noise is non negligible and may have a great impact on sensor performances in the two probe configuration was used.

3.2. Results

Preliminary results presented in Fig. 6 showed that the sensor can not be used in a two contact configuration. A four probe configuration must be used to ensure best signal to noise ratio. Moreover, the metallic pads used for the voltage contacts have also to be placed in a correct manner in order to avoid any possible current path through this metallic contact. As a consequence, metallic voltage pads should not be placed onto the line (like in Transmission Line Measurement (TLM) patterns for instance) but on the side of the line in order to achieve a low frequency noise level sensor.

In these conditions, Fig. 7 shows the voltage noise spectral density measured for a typical device ($W=50\text{ }\mu\text{m}$ and $L=300\text{ }\mu\text{m}$) in four probe configuration for different values of the bias current I in the device. As expected, the white noise level does not depend on the bias current but the $1/f$ noise increases with bias current.

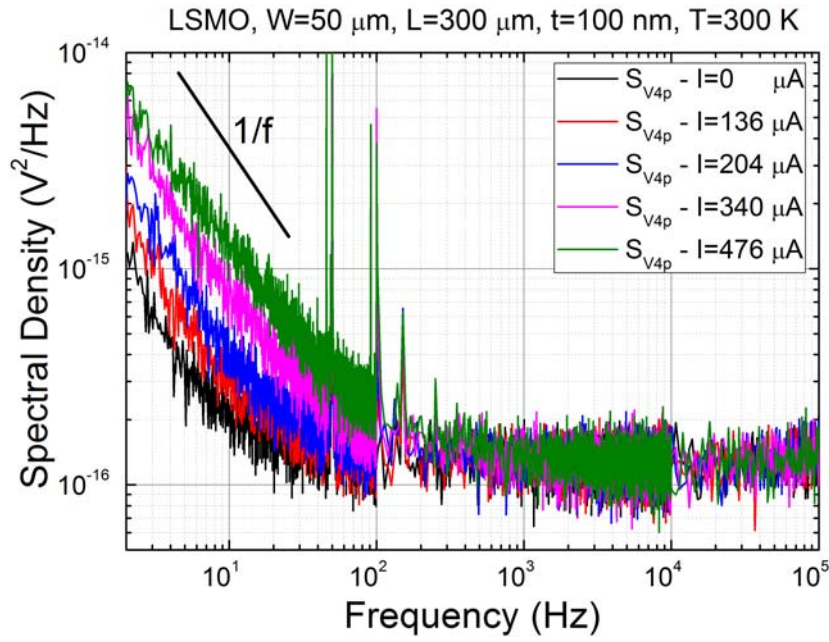


Fig. 7. Noise spectral density measured in the four probe configuration at different bias currents. White noise does not depend on the bias point on the contrary to 1/f noise.

Following the geometrical behaviour reported in homogeneous sample, the 1/f noise level at 1 Hz is in the inverse ratio of the device volume $W \times L \times t$ [14]. A deviation from this relation can be explained by non homogeneous sample. Finally, the noise spectral density of the sample in the four probe configuration $S_{V4p}(f)$ can be written as follow:

$$S_{V4P}(f) = \frac{K_{1/f}}{f \times W \times L \times t} \times V^2 + \frac{4 \times k_B \times T \times \rho \times L}{W \times t}, \quad (1)$$

where ρ is the film electrical resistivity (typical value is in the 2-4 m Ω ·cm for LSMO at 300 K) and $K_{1/f}$ is a material characteristic independent of the geometry that quantify the value of the $K_{1/f}$ noise level. In this sample, $K_{1/f}$ is found around $1 \times 10^{-30} \text{ m}^3$. As reported in [8], this $K_{1/f}$ value is among the lowest reported values for LSMO samples and is comparable with values reported for integrated silicon resistances.

Fig. 8 shows the noise spectral density at 1 Hz versus the sample voltage. In this log-log graph a slope equal to 2 was found, as expected from equation (1) for a quadratic dependence of the noise spectral density S_{V4p} with the sample voltage V . This verified quadratic dependence is an indication that the sample and the noise sources are homogeneous. Equation (1) also clearly shows that length and bias dependency of the noise are completely different in the low frequency and white noise ranges. These discussions will be extended in the next section in the framework of sensor performance analysis.

4. Sensor Performances

In this section, the performances in terms of signal-to-noise ratio will be presented and discussed in the case of thermometers and magnetoresistance sensors.

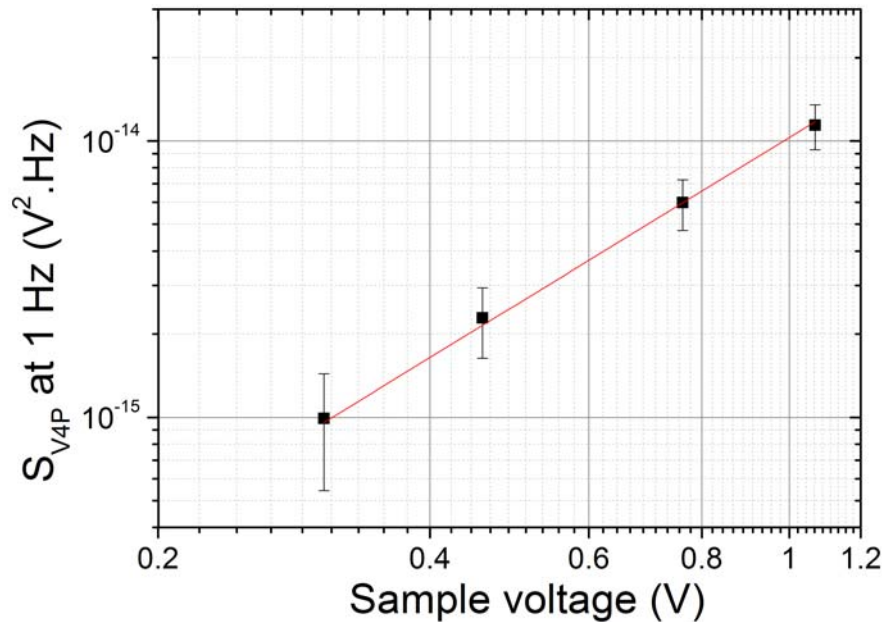


Fig. 8. Noise spectral density at 1 Hz versus the sample voltage.

4.1. Background

To use the devices as sensors, a current source is connected and the voltage across the sensor is measured. A four probe configuration will be used to avoid the current contact noise contribution. Either the temperature T or the magnetic field $\mu_0 H$ are the measurand. For these theoretical derivations, the measurand will be noted M and the relative sensitivity β_M , defined in the following equation, will be used:

$$\beta_M = \frac{1}{R} \times \left(\frac{dR}{dM} \right)_{M_0}, \quad (2)$$

where M_0 is the DC value of the measurand for which the relative sensitivity is estimated. The equivalent input sensor noise $S_M(f)$ is given by the ratio of the voltage noise spectral density of the sensor $S_V(f)$ (given by $S_{V4p}(f)$ in the case of our LSMO samples in the previous sample) over the square of the voltage sensitivity at M_0 given by $(dV/dM = V \times \beta_M)$. Using equation (1), it follows that $S_M(f)$ finally writes:

$$S_M(f) = \frac{S_V(f)}{(dV/dM)^2} = \frac{1}{\beta_M^2} \left(\frac{K_{1/f}}{f \times W \times L \times t} + \frac{4 \times k_B \times T \times \rho \times L}{V^2 \times t \times W} \right) \quad (3)$$

In order to obtain the smallest noise sensor, this equation shows that in addition to large sensitivity values, low value of the $1/f$ noise parameter $K_{1/f}$ and low value of the electrical resistivity are first required. Two geometrical and bias dependencies can then be distinguished:

- in the low frequency part where $1/f$ noise dominates, the equivalent input sensor noise does not depend on the bias and the sample should have the largest volume $W \times L \times t$;
- in the white noise range of frequencies, the equivalent input sensor noise decreases with the square of the bias voltage. The geometry should have the smallest ratio value L/W and the sensor should also be as thick as possible.

All these considerations obviously do not take into account other constraints such as frequency bandwidth or cost, which usually leads to opposite conclusions in term of device volume or size. The above noise analysis is illustrated in the next sections for LSMO thermometers and LSMO magnetoresistance sensors ($L=300\text{ }\mu\text{m}$, $W=150\text{ }\mu\text{m}$) considering $1/f$ noise.

4.2. Thermometers

LSMO electrical resistivity ρ and relative temperature sensitivity β_T (also called TCR for Temperature Coefficient of the Resistance) in case of thermometers versus temperature T are shown in Fig. 9. In this kind of material, a transition from metallic to insulator behaviour occurs for temperature close to room temperature as already reported [15]. In this sample, the maximum value of β_T is found for temperature close to 330 K, and is reported in Table 1.

Table 1. Typical electrical characteristics and noise properties of the film used for the estimation of the signal-to-noise ratio. The values are given for a device length and width of $300\text{ }\mu\text{m}$ and $50\text{ }\mu\text{m}$, respectively.

Parameter	Value
$K_{1/f}(\text{m}^3)$ at 300 K	1×10^{-30}
$\rho (\Omega \cdot \text{m})$ at 300 K and at 330 K	3.5×10^{-5} (300K), 6.3×10^{-5} (330K)
$\beta_{T\text{MAX}}$ at 330 K (K^{-1})	2.7×10^{-2}
$\beta_{H\text{MAX}}$ at 300 K (T^{-1})	~ 1

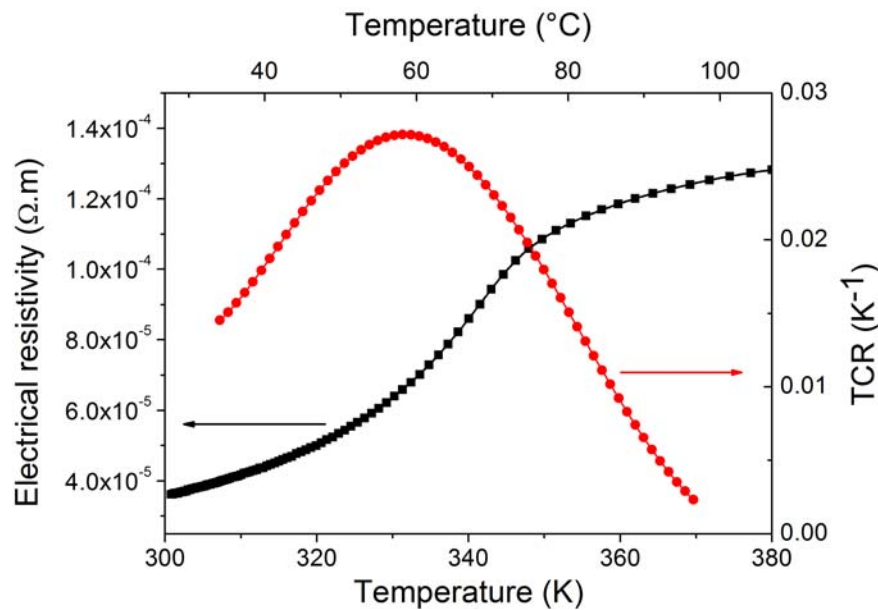


Fig. 9. LSMO electrical resistivity ρ (square symbols, left axis) and relative temperature sensitivity β_T (circle symbols, right axis) versus temperature T in the 300-380 K range for a line with $W=50\text{ }\mu\text{m}$ and $L=300\text{ }\mu\text{m}$. The maximum sensitivity is found around 330 K where $\beta_T = 2.7 \times 10^{-2} \text{ K}^{-1}$.

4.3. Magnetoresistance Sensors

LSMO electrical resistance and relative magnetic field sensitivity β_H as a function of the magnetic field $\mu_0 H$ are shown in Fig. 10. Due to the ferromagnetic behaviour of LSMO at room temperature, a magnetoresistance effect is observed. Two kinds of effect can be distinguished:

- i) a Colossal MagnetoResistance effect (CMR) for magnetic field values greater than 2 mT [16-18], and ii) a low field magnetoresistance effect for magnetic field values close to 0.5 mT.

The first one leads to a small sensitivity with no interesting sensor applications. The second one is related to the magnetization reversal [18-20]. It gives two peaks in the R versus $\mu_0 H$ characteristic and a relatively high value of the relative magnetic field sensitivity (absolute typical values around 1 T^{-1} for an operation point around 1 mT) at room temperature (Table 1).

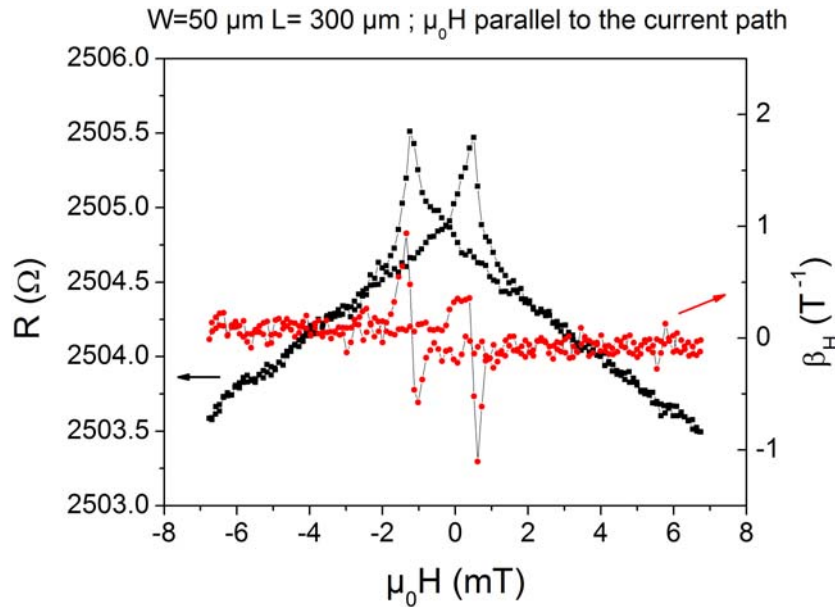


Fig. 10. LSMO electrical resistance R (square symbols, left axis) and relative magnetic field sensitivity β_H (circle symbols, right axis) as a function of the magnetic field $\mu_0 H$ at room temperature for a line with $W=50 \mu\text{m}$ and $L=300 \mu\text{m}$. Magnetic field is parallel to the current direction. Sensitivity maxima observed at low magnetic field are related to the magnetization reversal in the film.

4.4. Discussion

In this discussion, it will be assumed that the thermometer or the magnetoresistance is connected in four probe configuration and that the device geometry leads to the smallest value of $1/f$ noise. The noise performances in terms of equivalent input sensor noise values of DC current will be calculated with the data in Table 2 for three values of the DC current $I = 100 \mu\text{A}$, $I = 1 \text{ mA}$ and $I = 5 \text{ mA}$.

Table 2 summarizes the results for a $150 \mu\text{m}$ wide and $300 \mu\text{m}$ long thermometer or magnetoresistance at optimal operating point (330 K for the thermometer, 300 K and 0.1 mT for the magnetoresistance). In this table, the equivalent input sensor noise has been calculated at two frequencies (30 Hz and 10 kHz) to distinguish between the low frequency domain where $1/f$ noise dominates and the white noise domain.

The equivalent input sensor spectral densities $S_T(f)$ (also called NET for Noise Equivalent Temperature) and $S_H(f)$ calculated using equation 3 and data from table 1 are shown in Fig. 11. As expected, the spectral density at low frequency does not depend on the bias when $1/f$ noise dominates. On the contrary, at high frequency, the noise level is directly related to the applied bias current. From this figure, it appears that ultimate performances can be achieved at highest current. This remark has obviously to be moderated by the fact that self heating effects occur for too high current values so that the noise performances will be discussed in the following for a bias current limited to $100 \mu\text{A}$. At low

bias current, the $1/f$ noise contribution is negligible. In this LSMO sample, due to the low value of the $1/f$ noise level, the noise spectral density mainly consists in white noise even at a bias current of about $300\text{ }\mu\text{A}$.

Table 2. Sensor performances for a $150\text{ }\mu\text{m}$ wide $300\text{ }\mu\text{m}$ long line at different bias current I .

(*) $R = 700\text{ }\Omega$ at 300 K , (**) $R = 1260\text{ }\Omega$ at 330 K .

Bias current I (mA)	0.1	1	5
$\frac{dV}{d(\mu_0 H)}$ at 300 K (mV/T) (*)	45.5	455	2275
$\sqrt{S_H(f)}$ at 300 K ($\text{nT}\cdot\text{Hz}^{-0.5}$)			
$f = 30\text{ Hz}$	78	8.6	4.4
$f = 10\text{ kHz}$	75	7.5	1
$\frac{dV}{dT}$ at 330 K (mV/K) (**)	3.4	34	170
$\sqrt{S_T(f)}$ at 330 K ($\text{nK}\cdot\text{Hz}^{-0.5}$)			
$f = 30\text{ Hz}$	1400	170	100
$f = 10\text{ kHz}$	1400	140	30

The reported NET values are lower (at least one magnitude order) than the one of other uncooled thermometers such as amorphous semiconductors, vanadium oxides, etc. or the well-known Pt100 thermometer [8, 9]. This can easily be explained by the lower noise level of epitaxial manganites thin films compared to others. The results show that despite a quite small TCR value and thanks to a very low-noise level, LSMO thin films are real potential material for uncooled thermometry, as concluded previously by Lisauskas et al. for another manganite composition, namely $\text{La}_{0.7}(\text{Pb}_{1-x}\text{Sr}_x)_{0.3}\text{MnO}_3$ [21].

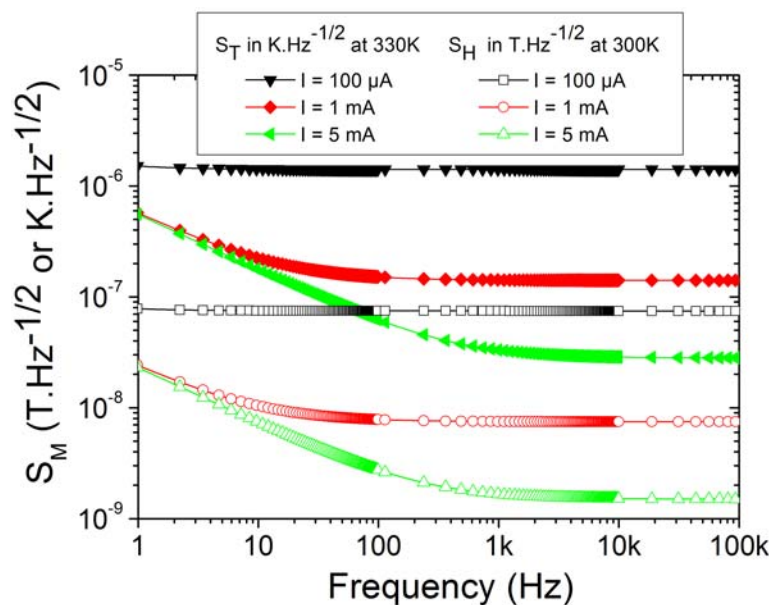


Fig. 11. Square root of the estimated equivalent input sensor spectral densities $S_T(f)$ (filled symbols) or $S_H(f)$ (open symbols) using equation (3) and the table 1 data for three values of the DC current I for a $150\text{ }\mu\text{m}$ width and $300\text{ }\mu\text{m}$ length sensor.

According to [22] where equivalent input sensor spectral densities $S_H(f)$ have been compared for various kinds of magnetic sensors, this LSMO magnetoresistance noise performances are better than Hall effect sensors. Equivalent input sensor spectral densities are only one order of magnitude higher than commercial Honeywell HMC1001 sensors [22-24]. These results are promising since the mask used was not optimized for sensor applications so that the sensitivity could be increased by changing the substrate type or the line geometry. Moreover, it has been demonstrated that LSMO can be deposited onto silicon substrate [25] without modifications of the magnetic properties: compatibility with the standard semiconductor used in the microelectronic industry has thus been demonstrated. This is another way to extend to "More than Moore" idea proposed by the International Roadmap for Semiconductor by the integration of manganese oxide.

5. Conclusion

In this paper, the potentialities of LSMO thin films as magnetic and temperature sensors at room temperature have been reported. It has been shown that a four probe configuration is required to remove the current contact noise that is often several orders of magnitude higher than the material noise. In such conditions, the performances of the room thermometers are in the state of the art for thermometers and that magnetoresistance exhibits noise performances one decade better than classical hall effect sensors.

Acknowledgements

The authors would like to thank C. Fur, J. Gasnier and S. Lebargy for technical assistance in sample fabrication and DC electrical transport measurements.

References

- [1]. T. Venkatesan, M. Rajeswari, Z. -W. Dong, S. B. Ogale, and R. Ramesh, Manganite-based devices: opportunities, bottlenecks and challenges, *Philos. Trans. R. Soc. London, Ser. A*, Vol. 356, No. 1742, 1998, pp. 1661–1680.
- [2]. M. Bibes, A. Barthélémy, Oxide spintronics, *IEEE Transactions on Electron Devices*, Vol. 54, No. 5, 2007, pp. 1003-1023.
- [3]. M. Rajeswari, A. Goyal, A. Raychaudhuri, M. Robson, G. Xiong, C. Kwon, R. Ramesh, R. Greene, T. Venkatesan, and S. Lakeou, 1/f electrical noise in epitaxial thin films of the manganite oxides $\text{La}_{0.67}\text{Ca}_{0.33}\text{MnO}_3$ and $\text{Pr}_{0.67}\text{Sr}_{0.33}\text{MnO}_3$, *Appl. Phys. Lett.*, Vol. 69, No. 6, 1996, pp. 851–853.
- [4]. B. Raquet, J. Coey, S. Wirth, and S. von Molnar, 1/f noise in the half-metallic oxides CrO_2 , Fe_3O_4 , and $\text{La}_{2/3}\text{Sr}_{1/3}\text{MnO}_3$, *Phys. Rev. B*, Vol. 59, No. 19, 1999, pp. 12435–12443.
- [5]. A. Lisauskas, S. Khartsev, and A. Grishin, Studies of 1/f Noise in $\text{La}_{1-x}\text{Sr}_x\text{MnO}_3$ (M= Sr,Pb) Epitaxial Thin Films, *J. Low Temp. Phys.*, Vol. 117, No. 5, 1999, pp. 1647–1651.
- [6]. A. Palanisami, R. Merithew, M. Weissman, M. Warusawithana, F. Hess, and J. Eckstein, Small conductance fluctuations in a second-order colossal magnetoresistive transition, *Phys. Rev. B*, Vol. 66, No. 9, 2002, p. 92407.
- [7]. K. Han, Q. Huang, P. Ong, and C. Ong, Low-frequency noise in $\text{La}_{0.7}\text{Sr}_{0.3}\text{Mn}_{1-x}\text{FeO}_3$ thin films, *J. Phys. Condens. Matter*, Vol. 14, 2002, p. 6619.
- [8]. L. Méchin, J.-M. Routoure, S. Mercone, F. Yang, S. Flament, and R. Chakalov, 1/f noise in patterned $\text{La}_{0.7}\text{Sr}_{0.3}\text{MnO}_3$ thin films in the 300–400 K range, *J. Appl. Phys*, Vol. 103, 2008, p. 083709.
- [9]. F. Yang, L. Méchin, J.-M. Routoure, B. Guillet, and R. A. Chakalov, Low-noise $\text{La}_{0.7}\text{Sr}_{0.3}\text{MnO}_3$ thermometers for uncooled bolometric applications, *J. Appl. Phys*, Vol. 99, No. 2, 2006, p. 024903.
- [10]. L. Méchin, J.-M. Routoure, B. Guillet, F. Yang, S. Flament, D. Robbes, and R. Chakalov, Uncooled bolometer response of a low noise $\text{La}_{2/3}\text{Sr}_{1/3}\text{MnO}_3$ thin film, *Appl. Phys. Lett.*, Vol. 87, 2005, p. 204103.
- [11]. J.-M. Routoure, D. Fadil, S. Flament, and L. Méchin, A low-noise high output impedance DC current

- source, in *Proceedings of the 19th International Conference on Noise and Fluctuations (ICNF' 2007)*, AIP Conference Proceedings, Vol. 922, No. 1, 2007, pp. 419–424.
- [12].C. Barone, A. Galdi, S. Pagano, O. Quaranta, L. Méchin, J. Routoure, and P. Perna, Experimental technique for reducing contact and background noise in voltage spectral density measurements, *Rev. Sci. Instrum.*, Vol. 78, 2007, p. 093905.
- [13].C. Barone, S. Pagano, L. Méchin, J.-M. Routoure, P. Orgiani, and L. Maritato, Apparent volume dependence of $1/f$ noise in thin film structures: Role of contacts, *Rev. Sci. Instrum.*, Vol. 79, 2008, p. 053908.
- [14].F. N. Hooge, $1/f$ noise is no surface effect, *Phys. Lett.*, 29, A, 3, 1969, p. 139.
- [15].A. Urushibara, Y. Moritomo, T. Arima, A. Asamitsu, G. Kido, and Y. Tokura, Insulator-metal transition and giant magnetoresistance in $\text{La}_{1-x}\text{Sr}_x\text{MnO}_3$, *Phys. Rev. B*, Vol. 51, No. 20, 1995, pp. 14103–14109.
- [16].J. O'Donnell, M. Onellion, M. Rzechowski, J. Eckstein, and I. Bozovic, Low-field magnetoresistance in tetragonal $\text{La}_{1-x}\text{Ca}_x\text{MnO}_3$ sfilms, *Phys. Rev. B*, Vol. 55, No. 9, 1997, p. 5873.
- [17].J. O'Donnell, M. Onellion, M. Rzechowski, J. Eckstein, and I. Bozovic, Anisotropic properties of molecular beam epitaxygrown colossal magnetoresistance manganite thin films, *J. Appl. Phys*, Vol. 81, 1997, p. 4961.
- [18].P K Siwach, , H K Singh and O N Srivastava, Low field magnetotransport in manganites, *J. Phys.: Condens. Matter*, 20, 273201, 2008, pp. 1-43.
- [19].M. Saïb, M. Belmeguenai, L. Méchin, D. Bloyet, and S. Flament, Magnetization reversal in patterned $\text{La}_{0.67}\text{Sr}_{0.33}\text{MnO}_3$ thin films by magneto-optical Kerr imaging, *J. Appl. Phys*, Vol. 103, No. 11, 2008, p. 113905.
- [20].P. Perna, L. Méchin, M. Saïb, S. Flament, Imaging the magnetization reversal of step-induced uniaxial magnetic anisotropy in vicinal epitaxial $\text{La}_{0.7}\text{Sr}_{0.3}\text{MnO}_3$ films, *New Journal of Physics*, 12, 2010, p. 103033.
- [21].A. Lisauskas, J. Bačck, S. I. Khartsev, and A. M. Grishin, Colossal magnetoresistive $\text{La}_{0.7}(\text{Pb}_{1-x}\text{Sr}_x)_{0.3}\text{MnO}_3$ films for bolometer and magnetic sensor applications, *J. Appl. Phys.*, Vol. 89, No. 11, 2001, p. 6961.
- [22].T. McGuire and R. Potter, Anisotropic magnetoresistance in ferromagnetic 3d alloys, *IEEE Trans. Magn.*, Vol. 11, No. 4, 1975, pp. 1018– 1038.
- [23].A. Jander, C. Smith, and R. Schneider, Magnetoresistive sensors for nondestructive evaluation (Invited Paper) (Proceedings Paper), in *Proceeding of the 10th SPIE International Symposium, Nondestructive Evaluation for Health Monitoring and Diagnostics, Conference 5770*, 2005.
- [24].M. Díaz-Michelena, Small magnetic sensors for space applications, *Sensors*, Vol. 9, No. 4, 2009, pp. 2271–2288.
- [25].M. Belmeguenai, S. Mercone, C. Adamo, L. Méchin, C. Fur, P. Monod, P. Moch, and D. G. Schlom, Temperature dependence of magnetic properties of $\text{La}_{0.7}\text{Sr}_{0.3}\text{MnO}_3$ / SrTiO_3 thin films on silicon substrates, *Phys. Rev. B*, Vol. 81, No. 5, 2010, p. 054410.

Guide for Contributors

Aims and Scope

Sensors & Transducers Journal (ISSN 1726-5479) provides an advanced forum for the science and technology of physical, chemical sensors and biosensors. It publishes state-of-the-art reviews, regular research and application specific papers, short notes, letters to Editor and sensors related books reviews as well as academic, practical and commercial information of interest to its readership. Because of it is a peer reviewed international journal, papers rapidly published in *Sensors & Transducers Journal* will receive a very high publicity. The journal is published monthly as twelve issues per year by International Frequency Sensor Association (IFSA). In addition, some special sponsored and conference issues published annually. *Sensors & Transducers Journal* is indexed and abstracted very quickly by Chemical Abstracts, IndexCopernicus Journals Master List, Open J-Gate, Google Scholar, etc. Since 2011 the journal is covered and indexed (including a Scopus, Embase, Engineering Village and Reaxys) in Elsevier products.

Topics Covered

Contributions are invited on all aspects of research, development and application of the science and technology of sensors, transducers and sensor instrumentations. Topics include, but are not restricted to:

- Physical, chemical and biosensors;
- Digital, frequency, period, duty-cycle, time interval, PWM, pulse number output sensors and transducers;
- Theory, principles, effects, design, standardization and modeling;
- Smart sensors and systems;
- Sensor instrumentation;
- Virtual instruments;
- Sensors interfaces, buses and networks;
- Signal processing;
- Frequency (period, duty-cycle)-to-digital converters, ADC;
- Technologies and materials;
- Nanosensors;
- Microsystems;
- Applications.

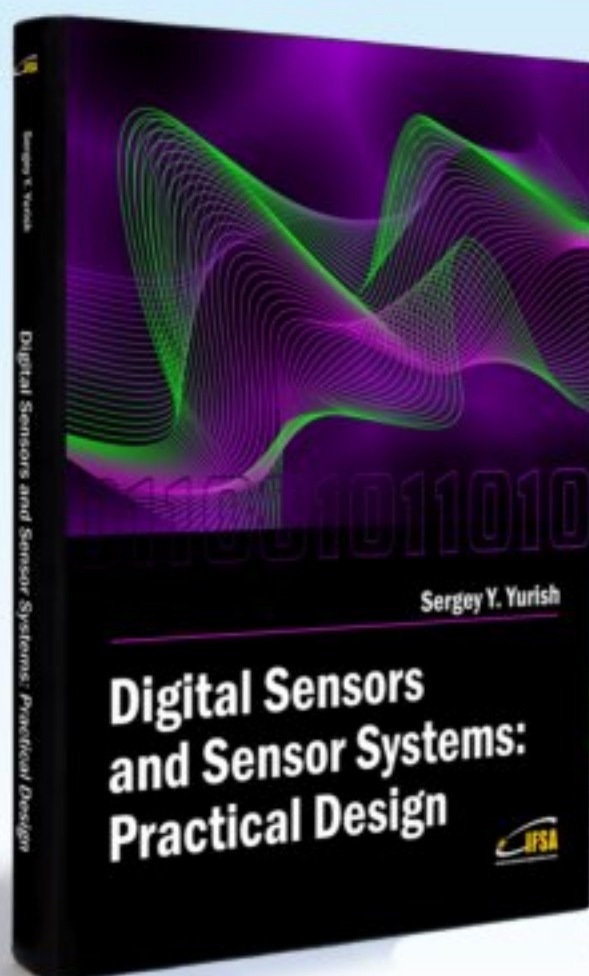
Submission of papers

Articles should be written in English. Authors are invited to submit by e-mail editor@sensorsportal.com 8-14 pages article (including abstract, illustrations (color or grayscale), photos and references) in both: MS Word (doc) and Acrobat (pdf) formats. Detailed preparation instructions, paper example and template of manuscript are available from the journal's webpage: <http://www.sensorsportal.com/HTML/DIGEST/Submission.htm> Authors must follow the instructions strictly when submitting their manuscripts.

Advertising Information

Advertising orders and enquires may be sent to sales@sensorsportal.com Please download also our media kit: http://www.sensorsportal.com/DOWNLOADS/Media_Kit_2012.pdf

Digital Sensors and Sensor Systems: Practical Design will greatly benefit undergraduate and at PhD students, engineers, scientists and researchers in both industry and academia. It is especially suited as a reference guide for practitioners, working for Original Equipment Manufacturers (OEM) electronics market (electronics/hardware), sensor industry, and using commercial-off-the-shelf components, as well as anyone facing new challenges in technologies, and those involved in the design and creation of new digital sensors and sensor systems, including smart and/or intelligent sensors for physical or chemical, electrical or non-electrical quantities.



"It is an outstanding and most completed practical guide about how to deal with frequency, period, duty-cycle, time interval, pulse width modulated, phase-shift and pulse number output sensors and transducers and quickly create various low-cost digital sensors and sensor systems ..." (from a review)

Order online:

http://www.sensorsportal.com/HTML/BOOKSTORE/Digital_Sensors.htm



www.sensorsportal.com